

**Measurement of the  $t\bar{t}$  Production Cross-section  
at  $\sqrt{s} = 1.96$  TeV in Electron Muon Final States Using  $1.05 \text{ fb}^{-1}$**

The DØ Collaboration  
(Dated: March 7, 2007)

We present a measurement of the top quark pair ( $t\bar{t}$ ) production cross section in  $p\bar{p}$  collisions at  $\sqrt{s} = 1.96$  TeV using events in the  $e\mu$  final state. This analysis utilizes an integrated luminosity of  $1.05 \text{ fb}^{-1}$  collected with the DØ detector at the Fermilab Tevatron collider. The measured cross section in this channel for a top mass of 175 GeV is:

$$e\mu : \quad \sigma_{t\bar{t}} = 6.1_{-1.2}^{+1.4} (\text{stat}) \quad {}_{-0.7}^{+0.8} (\text{syst}) \pm 0.4 (\text{lumi}) \text{ pb.}$$

*Preliminary Results for Winter 2007 Conferences*

## I. INTRODUCTION

The top quark is the heaviest fermion, and its mass could allow its decay into exotic particles, e.g. a charged Higgs boson [1]. The inclusive top pair ( $t\bar{t}$ ) production cross section ( $\sigma_{t\bar{t}}$ ) can be computed from individual  $t\bar{t}$  decay channels and their predicted standard model branching ratios. Exotic top decays would lead to different values of the inclusive top pair production cross section in the different channels. It is therefore important to precisely measure  $\sigma_{t\bar{t}}$  in all channels and compare it with the standard model prediction. Within the standard model each top quark of a  $t\bar{t}$  pair is expected to decay approximately 99.8% of the time to a  $W$  boson and a  $b$  quark [2]. Dilepton final states arise when both  $W$  bosons decay leptonically and occur along with two energetic jets resulting from the hadronization of the  $b$  quarks and accompanied by missing transverse energy ( $\cancel{E}_T$ ) from the high transverse momentum ( $p_T$ ) neutrinos. For the  $e^\pm\mu^\mp$  channel, the corresponding standard model  $t\bar{t}$  branching fraction is 3.15% [2].

The ( $t\bar{t}$ ) production cross section in  $p\bar{p}$  collisions has been measured in the  $e^\pm\mu^\mp$  final state using the dataset provided by the Run II of the Tevatron [3]. In the present paper we update the  $D\bar{O}$  measurement in the  $e^\pm\mu^\mp$  channel using data taken in the period between April 2002 and February 2006. The measured luminosity for this channel after data quality selection is  $1.05 \text{ fb}^{-1}$  [4].

## II. LEPTON AND JET IDENTIFICATION

The  $D\bar{O}$  detector has a silicon microstrip tracker and a central fiber tracker located within a 2 T superconducting solenoidal magnet [5]. The surrounding liquid-argon/uranium sampling calorimeter has a central cryostat covering pseudo-rapidities  $|\eta|$  up to 1.1 [6], and two end cryostats extending coverage to  $|\eta| \approx 4$  [7]. A muon system [8] resides beyond the calorimetry, and consists of a layer of tracking detectors and scintillation trigger counters before 1.8 T toroids, followed by two similar layers after the toroids. Luminosity is measured using plastic scintillator arrays located in front of the end cryostats.

Electrons are identified as clusters of calorimeter cells in a cone of size  $\Delta R \equiv \sqrt{\Delta\phi^2 + \Delta\eta^2} = 0.4$ . Electron candidates are required to have a large fraction of their energy deposited in the electromagnetic layers of the calorimeter. The clusters are required to be isolated from hadronic, to have a matching charged track in the central tracking system and to have a shower shape consistent with that of an electron. Before the shower shape requirement electron candidates are referred to as “loose electrons”. We use both central ( $|\eta| < 1.1$ ) and forward ( $1.5 < |\eta| < 2.5$ ) electron candidates. We require the electrons to be selected by a likelihood discriminant that combines information both from the central tracking system and the calorimeter in order to select prompt electrons. Such electrons are referred to as “tight electrons”.

Muons are comprised of a track segment in the inner muon layer matching a segment formed from hits in the outer two muon layers. A track in the central tracking system must also match the muon identified in the muon system track, and the overall track  $\chi^2$  must be smaller than 4. To reject cosmic muons we apply cuts on the time of arrival of the muon track at the different layers of scintillators in the muon system. All muons must be found in  $|\eta| < 2.0$ . Muons supposedly originating from  $W$  (or  $Z$ ) decay are identified using two isolation criteria: *i*) the energy deposited in the calorimeter in a hollow cone around the muon is smaller than 15% of the energy of the muon itself (this fraction is referred to as “calorimeter isolation”), *ii*) the scalar sum of the momenta of the charged tracks surrounding the muon track in the central tracking system is smaller than 15% of the muon track  $p_T$  (this fraction is referred to as “tracker isolation”). To select prompt muons we also require that the distance of closest approach of the muon track with respect to the primary vertex is smaller than 0.02 cm for a muon track with a hit in the silicon microstrip tracker and smaller than 0.2 cm for a muon track without a hit in the silicon microstrip tracker.

Jets are reconstructed with a fixed cone of radius,  $\Delta R = 0.5$  [9] and must be confirmed by the independent calorimeter trigger readout. Jet energy calibration is applied to the jets [10]. The  $\cancel{E}_T$  is equal in magnitude and opposite in direction to the vector sum of the transverse energies in all calorimeter cells for which the energy is significantly above the noise. The transverse momenta of electrons and isolated muons are taken into account in the calculation of  $\cancel{E}_T$  as well as the jet energy calibration.

## III. EVENT SELECTIONS

We select events requiring that they pass an  $e\mu$  trigger. This  $e\mu$  trigger require a muon with a typical  $p_T$  threshold of 5 GeV, an electromagnetic object with a typical threshold of  $E_T = 12$  GeV as well as a track with  $p_T > 5$  GeV. Given the typical  $p_T$  for both signal and background processes we are dealing with, the trigger efficiency is found to be on the plateau. The trigger efficiency for  $t\bar{t}$  events is measured to be 86%.

We select events offline with at least one jet with  $p_T^j > 20$  GeV and  $|\eta| < 2.5$  [6], one electron and one muon both with  $p_T^\ell > 15$  GeV. Muons are accepted in the region  $|\eta| < 2.0$ , while electrons must be within  $|\eta| < 1.1$  or  $1.5 < |\eta| < 2.5$ . The electron and the muon are required to be of opposite charge. The final selection requires  $H_T^i = p_T^{\ell_1} + \Sigma(p_T^j) > 115$  GeV, where  $p_T^{\ell_1}$  denotes the  $p_T$  of the leading lepton. This cut effectively rejects the largest backgrounds for this final state which arise from  $Z/\gamma^* \rightarrow \tau^+\tau^-$  and diboson production.

#### IV. SIGNAL EFFICIENCY

In order to compute the acceptances and efficiencies for the signal we generate  $t\bar{t}$  events at  $\sqrt{s} = 1.96$  TeV using the ALPGEN [11] matrix element generator assuming a top mass  $m_{top}$  of 175 GeV. These events are processed through PYTHIA [12] to provide fragmentation, hadronization and decays of short-lived particles. EVTGEN [13] is used to model the decays of  $b$  hadrons. The two  $W$ 's decay to two lepton-neutrino pairs, including all  $\tau$  final states. These events are processed through a full detector simulation using GEANT [14] providing tracking hits, calorimeter cell energy and muon hit information. Extra  $p\bar{p}$  interactions are added to all events subject to Poisson statistics given the instantaneous luminosities typically observed in the run. The same reconstruction is applied to data and Monte Carlo events.

#### V. BACKGROUND PROCESSES

Several background processes can fulfill the preselection criteria designed to select  $t\bar{t}$ . We distinguish two categories of backgrounds: “physics” and “instrumental”. Physics backgrounds are processes in which the charged leptons arise from electroweak boson decay. This signature arises from  $Z/\gamma^* \rightarrow \tau^+\tau^-$  where the  $\tau$  leptons decay leptonically, and  $WW/WZ$  (diboson) production. Instrumental backgrounds are defined as events in which a jet or a lepton within a jet is misidentified as an isolated lepton (fake).

##### A. Physics Backgrounds

The selection efficiencies for the physics backgrounds  $Z/\gamma^* \rightarrow \tau^+\tau^- \rightarrow e\mu$  are estimated using Monte Carlo samples generated by ALPGEN followed by PYTHIA while for  $WW/WZ$  they are estimated using PYTHIA. The  $Z/\gamma^* \rightarrow \tau^+\tau^-$  and diboson +  $\leq 2$  jets processes are generated at leading order (LO) and are scaled by the ratio of the next-to-next-to-leading order to LO inclusive cross sections [15, 16]. The correction leads to an increase of 38% for the  $Z/\gamma^* \rightarrow \tau^+\tau^-$  and of 40% for the diboson prediction. As the Z boson  $p_T$  is not properly described in the ALPGEN simulation, we reweighted the Z-boson  $p_T$  distribution for different jet multiplicity bins using  $Z \rightarrow e^+e^-$  data events.

##### B. Misidentified Electron Background

Misidentified electrons can arise from instrumental effects. Jets comprised essentially of a leading  $\pi^0/\eta$  and an overlapping or conversion-produced track can, for example, mimic an isolated high- $p_T$  electron. The amount of misidentified electron background is fitted to the observed distribution of electron likelihood in the data. To this end we first determine the shape of the electron likelihood for real electrons on a pure  $Z/\gamma^* \rightarrow e^+e^-$  sample. The shape of the electron likelihood for the misidentified electron background is determined in a sample dominated by misidentified electrons and selected in the following way. The muon is required to be anti-isolated (both calorimeter and tracker isolation greater than 20%) and the event must have  $\cancel{E}_T < 15$  GeV. The number of misidentified electrons in the selected sample is obtained by performing an extended unbinned likelihood fit to the observed distribution of electron likelihood in data. The likelihood is given by:

$$\mathcal{L} = \prod_{i=1}^N (n_e S(x_i) + n_{misid} B(x_i)) \frac{e^{-(n_e + n_{misid})}}{N!},$$

where  $i$  is an index that runs over all selected events,  $x_i$  is the corresponding observed value of the electron likelihood,  $N$  is the total number of selected events,  $n_e$  is the number of events with an isolated electron,  $n_{misid}$  is the number of events with a misidentified electron,  $S$  is the signal probability distribution function determined using real electrons and  $B$  is the background probability distribution function derived from the sample dominated by misidentified electrons.

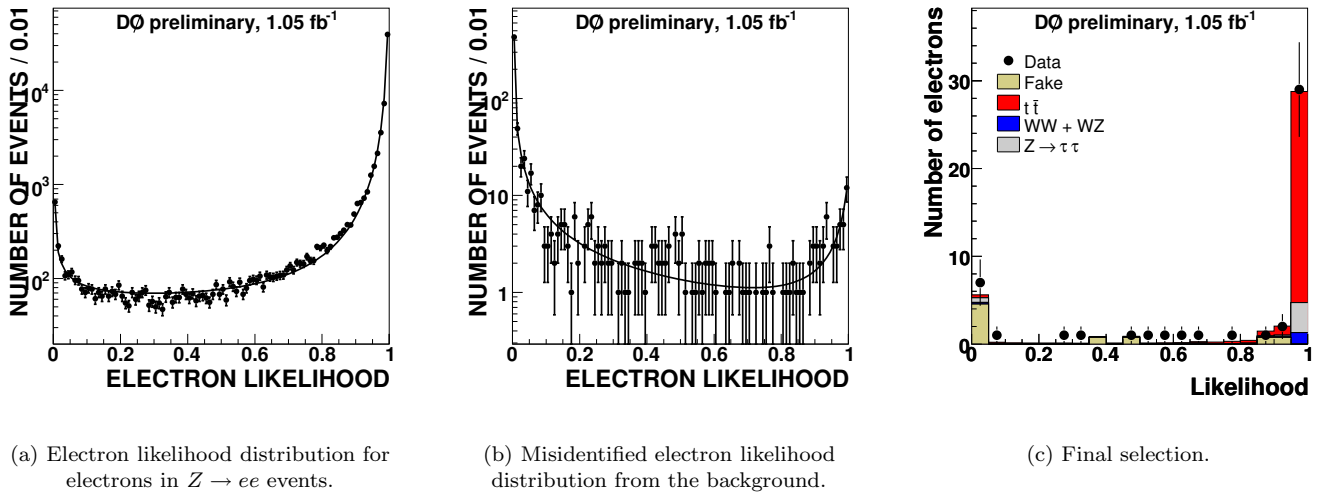


FIG. 1: Electron likelihood distributions.

Category	$e\mu$ ( $\geq 2$ jets)	$e\mu$ (1 jet)
Integrated luminosity, $pb^{-1}$	1046	1046
$WW/WZ$ and other MC	$1.4^{+0.6}_{-0.6}$	$3.4^{+1.4}_{-1.4}$
$Z/\gamma^*$	$3.6^{+0.7}_{-0.8}$	$5.5^{+0.8}_{-0.8}$
Instrumental leptons	$1.8^{+0.6}_{-0.6}$	$1.2^{+0.4}_{-0.4}$
<b>Total Bkg</b>	$6.7^{+1.2}_{-1.2}$	$10.2^{+1.8}_{-1.7}$
Signal efficiency, %	12.4	3.1
Expected signal	$28.6^{+2.1}_{-2.4}$	$7.1^{+0.6}_{-0.7}$
Total Sig. + Bkg.	$35.3^{+2.8}_{-3.2}$	$17.2^{+2.0}_{-2.1}$
Selected Events	32	16

TABLE 1: Expected background, observed and expected signal yields in both the 2 jet and 1 jet bins. The expected signal yield is derived assuming  $\sigma_{t\bar{t}} = 7$  pb. The errors on the yields are the quadratic sum of the statistical and systematic uncertainties.

Figure 1 shows the shapes of the electron likelihood discriminant distributions in the real and misidentified electron samples and the distribution observed in data.

Using this method, the number of misidentified electron in the final selection is found to be  $0.3^{+0.2}_{-0.1}$  requiring at least two jets and  $0.2^{+0.1}_{-0.1}$  requiring exactly one jet.

### C. Fake Isolated Muon Background

An isolated muon can be mimicked by a muon in a jet when the jet is not reconstructed. We measure the fraction  $f_\mu$  of muons that appear as isolated in a control sample dominated by fake isolated muons. The number of events with a fake isolated muon contributing to the final sample is computed as the number of events in a sample where the electron and the muon have the same sign and without any requirement on the muon isolation times the previously measured fraction  $f_\mu$ . This leads to the following estimation for the fake isolated muon background:  $1.5^{+0.6}_{-0.3}$  requiring at least two jets and  $1.0^{+0.4}_{-0.4}$  requiring exactly one jet.

## VI. PREDICTION AND OBSERVATION

In Table 1 we summarize the predicted and observed number of events requiring at least two jets and exactly one jet. The prediction for  $Z/\gamma^*$ , instrumental leptons and diboson backgrounds are also provided. Predicted and observed distributions for various event variables are shown in Fig 2.

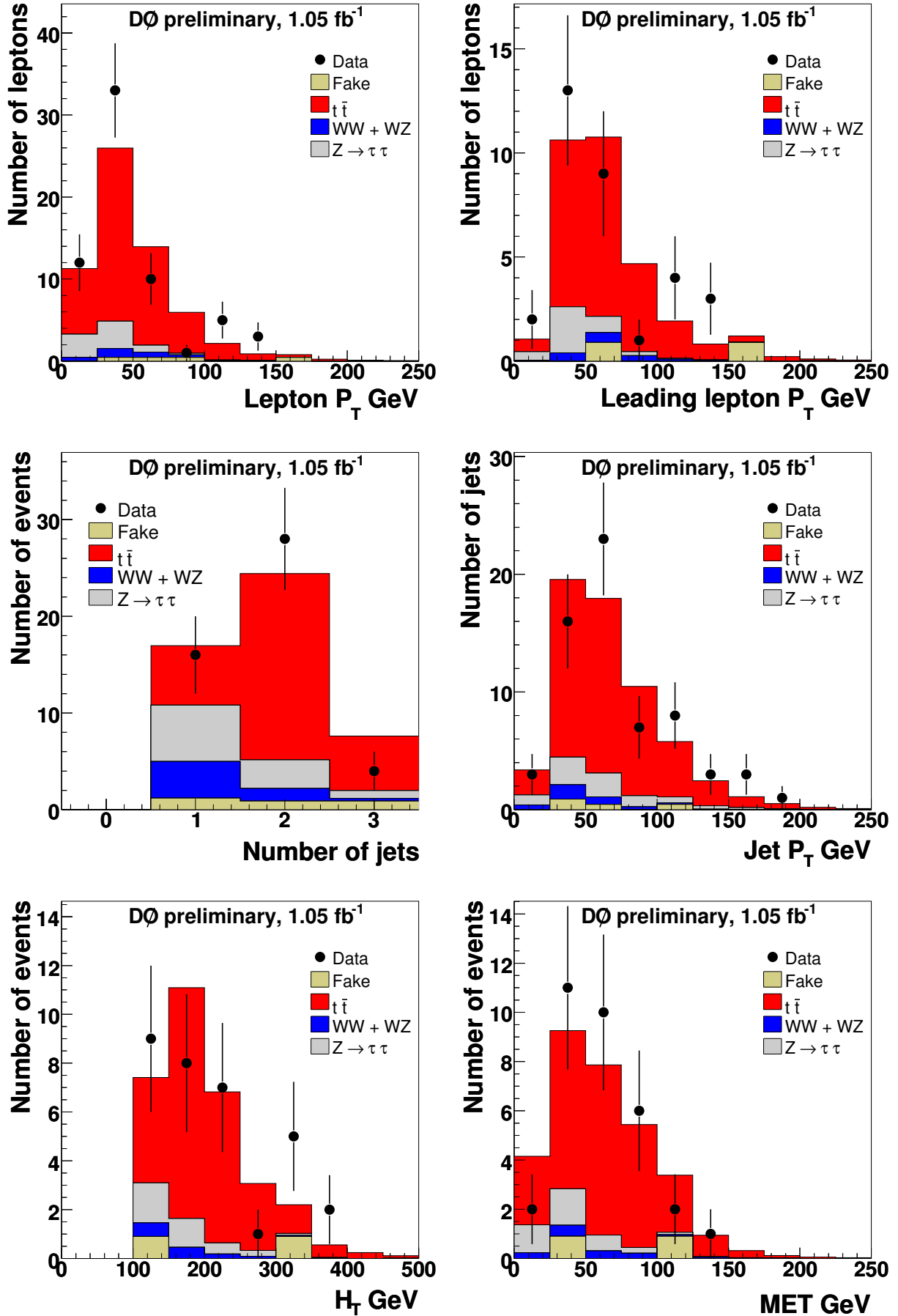


FIG. 2: Observed and predicted distributions for the various backgrounds and the signal after the final selection requiring at least two jets (except for the plot showing the number of jets that requires at least one jet). From top to bottom, lepton  $p_T$ , leading lepton  $p_T$ , number of jets, jet  $p_T$ , scalar sum of leading lepton and jets  $p_T$  ( $H_T$ ) and missing transverse energy (MET:  $\cancel{E}_T$ ).

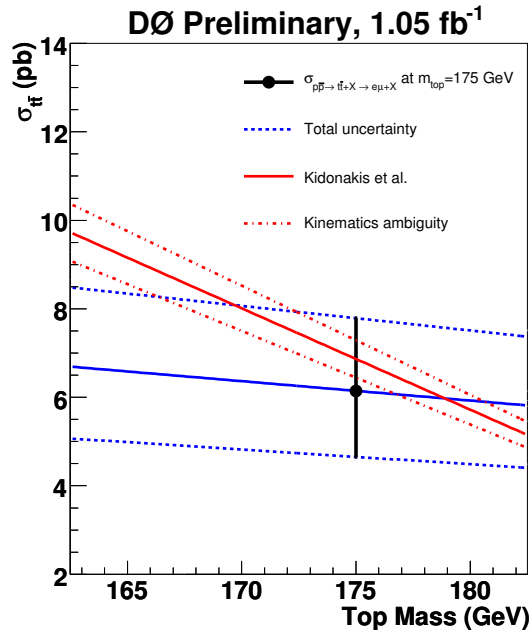


FIG. 3: Variation of the measured cross section (point) as a function of the top quark mass (blue lines). Also shown the theoretical prediction (red lines) from [18].

## VII. RESULTS

The  $t\bar{t}$  cross section is extracted by minimizing the negative log-likelihood function based on the Poisson probability to observe a number of events  $N_j^{obs}$  given the luminosity  $\mathcal{L}_j$ , branching fraction  $BR_j$ , efficiency  $\epsilon_j$  and a number of background events  $N_j^{bkg}$ :  $-\log L(\sigma_j, \{N_j^{obs}, N_j^{bkg}, BR_j, \mathcal{L}_j, \epsilon_j\})$ , while the combined cross section is measured by minimizing the sum of the negative log-likelihood functions for the 2 jet and 1 jet channels (see [17] for more details on the method).

The preliminary  $t\bar{t}$  production cross section at  $\sqrt{s} = 1.96$  TeV in the electron muon channel for the combined 1 jet and 2 jet channel and for a top mass of 175 GeV is measured to be:

$$e\mu: \quad \sigma_{t\bar{t}} = 6.1_{-1.2}^{+1.4} (\text{stat}) \pm 0.4 (\text{lumi}) \text{ pb}$$

in good agreement with the standard model prediction of  $6.77 \pm 0.42$  pb [18]. The variation of this measurement as a function of the top mass is shown in Fig 3.

The systematic uncertainty on the cross section measurement is obtained by varying the background and efficiencies, within their errors, with all the correlations between the different classes of background taken into account. The dominant systematic uncertainties are summarized in Table 2. The following main systematics have been studied.

- **Jet energy calibration:** The measured jet energies in the calorimeter are corrected for the response of the calorimeter, showering outside the jet cone and energy from underlying activity in the event [10]. The uncertainty on the jet energy calibration is propagated to the predicted background yields and the efficiency for the  $t\bar{t}$  signal.
- **Jet Reconstruction and jet resolution:** Jet reconstruction efficiency and jet resolution are determined in data and applied to Monte Carlo. Uncertainties related to the methods are propagated to signal and background predictions.
- **Primary vertex identification:** This uncertainty takes into account the difference observed in vertex distributions between data and Monte Carlo.
- **Lepton identification:** The lepton identification efficiencies are measured in the data using well understood processes. They are studied in various detector regions, and various jet environments. Residual deviations from unity of the ratio of data to Monte Carlo efficiencies are used as systematic uncertainties. The electron

TABLE 2: Summary of systematic uncertainties on  $\sigma_{t\bar{t}}$  for the selection requiring at least one jet.

Source	$\Delta\sigma_{t\bar{t}}$ (pb)
Jet energy calibration	+ 0.29 – 0.29
Jet identification	+ 0.05 – 0.05
PV identification	+ 0.28 – 0.18
Muon identification	+ 0.19 – 0.18
Electron identification	+ 0.47 – 0.42
Trigger	+ 0.20 – 0.19
Fakes	+ 0.25 – 0.30
MC normalization	+ 0.30 – 0.28
Other	+ 0.23 – 0.13
Subtotal	+ 0.82 – 0.74
Luminosity	$\pm 0.4$
Total	+ 0.91 – 0.84

identification systematic uncertainty is mainly due to the remaining dependency on the number of jets and is conservatively estimated to be around 5.5%.

- **Trigger efficiency:** Trigger efficiencies are derived in the data. They have uncertainties due to limited sample statistics. Various sources of bias are investigated, and the resulting variations in trigger efficiencies are used as systematic error.
- **Fake electron background:** The shape of the electron likelihood discriminant is used to fit the number of fake electrons in the selected final sample. The shape itself is found to be dependent on the electron  $p_T$  and the detector occupancy (number of jets). The number of fake electron is refitted with the various shapes to extract this systematic uncertainty on the background.
- **MC background normalization:** The ratio of the next-to-next-to-leading order to the leading order cross section used to scale the PYTHIA  $WW/WZ$  Monte Carlo cross sections is taken as systematic uncertainty for the diboson background. The systematic uncertainty on the  $Z/\gamma^* \rightarrow \tau^+\tau^-$  background normalization is evaluated varying the Z boson  $p_T$  reweighting function.

## VIII. ACKNOWLEDGEMENTS

We thank the staffs at Fermilab and collaborating institutions, and acknowledge support from the DOE and NSF (USA); CEA and CNRS/IN2P3 (France); FASI, Rosatom and RFBR (Russia); CAPES, CNPq, FAPERJ, FAPESP and FUNDUNESP (Brazil); DAE and DST (India); Colciencias (Colombia); CONACyT (Mexico); KRF and KOSEF (Korea); CONICET and UBACyT (Argentina); FOM (The Netherlands); PPARC (United Kingdom); MSMT (Czech Republic); CRC Program, CFI, NSERC and WestGrid Project (Canada); BMBF and DFG (Germany); SFI (Ireland); The Swedish Research Council (Sweden); Research Corporation; Alexander von Humboldt Foundation; and the Marie Curie Program.

- 
- [1] J.F. Gunion *et al.*, *The Higgs Hunters Guide* (Addison-Wesley, Redwood City, California, 1990), p. 200.
  - [2] S. Eidelman *et al.*, Phys. Lett. **592**, 1 (2004).
  - [3] CDF Collaboration, D. Acosta *et al.*, Phys. Rev. Lett. **93**, 142001 (2004); DØ Collaboration, V. Abazov *et al.*, Phys. Lett. B **626**, 55 (2005).
  - [4] T. Andeen *et al.*, FERMILAB-TM-2365-E (2006), in preparation.
  - [5] DØ Collaboration, V. Abazov *et al.*, *The Upgraded DØ Detector*, Nucl. Instrum. Meth. Phys. Res. A, **565**, 463 (2006).
  - [6] Rapidity  $y$  and pseudo-rapidity  $\eta$  are defined as functions of the polar angle  $\theta$  and parameter  $\beta$  as  $y(\theta, \beta) \equiv \frac{1}{2} \ln[(1 + \beta \cos\theta)/(1 - \beta \cos\theta)]$ ;  $\eta(\theta) \equiv y(\theta, 1)$ , where  $\beta$  is the ratio of a particle's momentum to its energy.
  - [7] DØ Collaboration, S. Abachi *et al.*, Nucl. Instrum. Meth. Phys. Res. A, **338** 185 (1994).
  - [8] V. Abazov *et al.*, *The muon system of the Run II D0 detector*, Nucl. Instr. and Meth. A **552**, 372 (2005).

- [9] Jets are defined using the iterative seed-based cone algorithm with  $\Delta\mathcal{R} = \sqrt{(\Delta\phi)^2 + (\Delta\eta)^2} = 0.5$  (where  $\phi$  is the azimuthal angle), including mid-points as described in Sec. 3.5 (p.47) of G. C. Blazey *et al.*, in *Proceedings of the Workshop: "QCD and Weak Boson Physics in Run II"*, edited by U. Baur, R. K. Ellis, and D. Zeppenfeld, FERMILAB-PUB-00-297 (2000).
- [10] DØ Collaboration, B. Abbott *et al.*, Nucl. Instrum. Meth. A **424**, 352 (1999).
- [11] M.L. Mangano *et al.*, *ALPGEN, a generator for hard multiparton processes in hadronic collisions*, JHEP **307**, 001 (2003), hep-ph/0206293.
- [12] <http://www.thep.lu.se/torbjorn/Pythia.html>  
T. Sjöstrand, T. Lönnblad, G. Miu, S. Mrenna and E. Norrbin, Comp. Phys. Commun. **135**, 238 (2001), hep-ph/0010017; see also T. Sjöstrand, T. Lönnblad, S. Mrenna and P. Skands, hep-ph/0308153.
- [13] D. J. Lange, Nucl. Instrum. Meth. Phys. Res. A **462**, 152 (2001).
- [14] R. Brun and F. Carminati, CERN Program Library Long Writeup W5013, 1993 (unpublished).
- [15] J.M. Campbell and R.K. Ellis, Phys. Rev. D **60**, 113006 (1999).
- [16] J.M. Campbell and R.K. Ellis, *MCFM - Monte Carlo for FeMtobarn processes*,  
<http://mcfm.fnal.gov>
- [17] DØ Collaboration, *Combined  $t\bar{t}$  Production Cross Section at  $\sqrt{s} = 1.96$  TeV in the Lepton+Jets and Dilepton Final States using Event Topology*, DØ Note 4906, August 2005.
- [18] R. Bonciani *et al.*, Nucl. Phys. **B529**, 424 (1998); N. Kidonakis and R. Vogt, Phys. Rev. D **68**, 114014 (2003); M. Cacciari *et al.*, JHEP **404**, 68 (2004).